Modeling flow and transport in highly heterogeneous three-dimensional aquifers: Ergodicity, Gaussianity, and anomalous behavior— 2. Approximate semianalytical solution

A. Fiori,[1] I. Janković,[2] and G. Dagan[3]

Received 21 November 2005; revised 3 March 2006; accepted 27 March 2006; published 24 May 2006.

[1] Flow and transport take place in a heterogeneous medium of lognormal distribution of the conductivity K. Flow is uniform in the mean, and the system is defined by U (mean velocity), σ_Y^2 (log conductivity variance), and integral scale I. Transport is analyzed in terms of the breakthrough curve of the solute, identical to the traveltime distribution, at control planes at distance x from the source. The "self-consistent" approximation is used, where the traveltime τ is approximated by the sum of τ pertinent to the different separate inclusions, and the neglected interaction between inclusions is accounted for by using the effective conductivity. The pdf $f(\tau, x)$, where x is the control plane distance, is derived by a simple convolution. It is found that $f(\tau, x)$ has an early arrival time portion that captures most of the mass and a long tail, which is related to the slow solute particles that are trapped in blocks of low K. The macrodispersivity is very large and is independent of x. The tail $f(\tau, x)$ is highly skewed, and only for extremely large x/I, depending on σ_Y^2, the plume becomes Gaussian. Comparison with numerical simulations shows very good agreement in spite of the absence of parameter fitting. It is found that finite plumes are not ergodic, and a cutoff of $f(\tau, x)$ is needed in order to fit the mass flux of a finite plume, depending on σ_Y^2 and x/I. The bulk of $f(\tau, x)$ can be approximated by a Gaussian shape, with fitted equivalent parameters. The issue of anomalous behavior is examined with the aid of the model.

Citation: Fiori, A., I. Janković, and G. Dagan (2006), Modeling flow and transport in highly heterogeneous three-dimensional aquifers: Ergodicity, Gaussianity, and anomalous behavior—2. Approximate semianalytical solution, *Water Resour. Res.*, *42*, W06D13, doi:10.1029/2005WR004752.

1. Introduction

[2] In Part 1 of this study [*Janković et al.*, 2006, hereinafter referred to as P1] we have analyzed longitudinal transport of a conservative solute in highly heterogeneous formations, by using the multi-indicator permeability model and highly accurate numerical simulations.

[3] The medium is made from an ensemble of densely packed spherical blocks (Figure 1 in P1) of uniform radius R, with log conductivity $Y = \ln K$ drawn independently from a normal distribution of variance σ_Y^2. The uniform matrix, filling the remaining 30% of the space is of conductivity K_{ef}, equal to the effective conductivity of the ensemble. The medium approximates at desired accuracy any formation of given stationary lognormal permeability distribution and finite integral scale. Flow is of uniform mean velocity U and a large plume is injected instantaneously in the plane $x = 0$ at $t = 0$. Flow and transport were solved in P1 numerically for highly heterogeneous formations ($\sigma_Y^2 = 2, 4, 8$). Longitudinal transport was analyzed with the aid of the solute mass flux $\mu(t, x)$ (equation (2) of P1) through CP (control planes) at x. The analysis of the numerically determined μ (Figure 3 in P1) and of the various temporal moments associated with it were the object of P1. For an ergodic plume it was shown that μ tends to the pdf (probability density function) $f(\tau, x)$ of the traveltime of a solute particle between the injection plane and the CP.

[4] In this part of the study we derive a simple, semi-analytical solution of the problem by using the model coined as "self-consistent" in our previous work [*Janković et al.*, 2003a; *Dagan et al.*, 2003; *Fiori et al.*, 2003a]. The basic idea is to use the simple solution of flow past an isolated spherical inclusion of arbitrary conductivity K that is submerged in a uniform matrix of conductivity K_0, with uniform flow U at infinity. Subsequently, the flow through the ensemble of spheres is approximated by the sum of the velocity perturbation fields associated with the different isolated spheres. This approximation is known as the "dilute" limit, as it neglects the interaction between neighboring inclusions. It is a first approximation in n, the volume density of the ensemble. We employed it, nevertheless, for the packing of highest density, with $n = 0.7$, for which spheres practically touch (Figure 1 in P1). We assumed that this is a valid approximation if we replace

[1]Dipartimento di Scienza dell'Ingegneria Civile, Universita' di Roma Tre, Rome, Italy.
[2]Department of Civil, Structural and Environmental Engineering, State University of New York at Buffalo, Buffalo, New York, USA.
[3]Department of Fluid Mechanics and Heat Transfer, Tel Aviv University, Tel Aviv, Israel.

0043-1397/06/2005WR004752$09.00

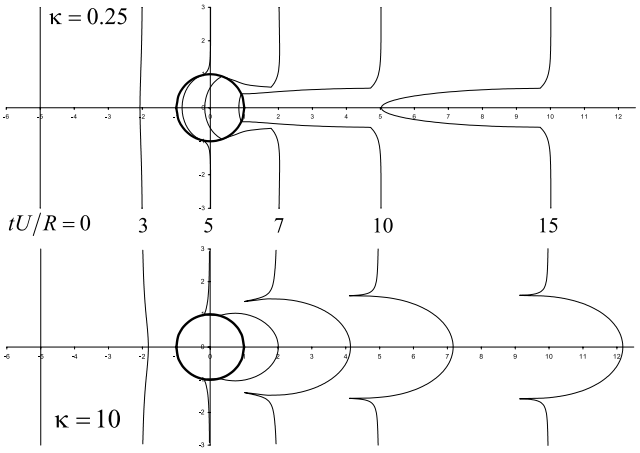

Figure 1. A few snapshots of a thin plume moving past a spherical inclusion for two conductivity ratios $\kappa = K/K_0$: $\kappa = 0.25$ and $\kappa = 10$.

K_0 by the effective conductivity of the medium K_{ef}. The intuitive justification [*Dagan*, 1979] was that since each inclusion is surrounded by a swarm of spheres of different conductivities, their collective impact can be determined by replacing them with a uniform medium of effective conductivity, that was derived by a self-consistency argument. The procedure was found to lead to an accurate value of K_{ef} for high values of the density n and variance σ_Y^2 [*Janković et al.*, 2003a].

[5] We derived the approximate solution of transport along the same lines, by solving first for a thin plume moving past an isolated inclusion, along the pioneering work of *Eames and Bush* [1999]. The spreading of the plume for the ensemble was determined again by superimposing the trajectory perturbations associated with the various inclusions. The longitudinal macrodispersivity derived by numerical simulations was compared with the semianalytical solution [*Janković et al.*, 2003b].

[6] In the present study we expand our previous work by using the same model, in order to determine the entire traveltime pdf, and the associated temporal moments, rather than the second and third spatial moments only. Furthermore, along the lines of P1, this is done for a different injection mode, of flux-proportional initial solute mass distribution, rather than a uniform one. The approach that we shall employ has some similarities with other methods developed in the past along the time domain random walk framework [*Bouchaud and Georges*, 1990; *Hughes*, 1996], for example the continuous time random walk [*Berkowitz and Scher*, 1995]. Alternative approaches addressing the same issues are the fractional ADE [*Cushman and Ginn*, 1993, 2000; *Benson et al.*, 2000] and the mass transfer model [see, e.g., *Harvey and Gorelick*, 2000]. However, the principal difference with existing methods is that the present approach is based on the solution of the flow problem for a given structure of the formation, while the solution of transport follows from it in a straightforward manner.

[7] Anticipating results, it is found that the semianalytical model leads to an accurate solution, as compared with the numerical one. This is particularly true for highly heterogeneous formations and for the tail of the traveltime pdf. The latter is related to the solute particles captured within inclusions of low K, in which the fluid velocity is very low and the residence time is very large. The magnitude of the interior velocity depends on the large contrast between the low value of K of the particular inclusion and that of the surrounding ones. In a previous study [*Janković et al.*, 2003a, Figure 5], the simplified model was found to capture accurately the dominant term of the interior velocity. It is emphasized that in this stage our main aim is to take advantage of the simple semianalytical model in order to acquire a better understanding of the mechanism of transport and of the limitations of numerical simulations.

[8] The plan of the paper is as follows: a summary of the development of the semianalytical model is presented in section 2. Section 3 is devoted to the derivation of the traveltime pdf. Section 4 deals with the comparison between the approximate solution and the numerical simulations of P1, and finally, a summarizing discussion of both parts is presented in section 5.

2. Development of the Semianalytical Model

2.1. Flow and Transport Past an Isolated Inclusion

[9] For the sake of completeness we recall a few previous results about flow and transport past an isolated inclusion of radius R and conductivity K, surrounded by an unbounded matrix of conductivity K_0. Uniform flow of velocity $\mathbf{U}(U, 0, 0)$ is applied at infinity. The well-known solution of the velocity field is

$$\mathbf{u}^{ex} = \nabla\phi^{ex} \quad ; \quad \phi^{ex} = U\frac{2(1-\kappa)}{2+\kappa}\frac{R^3(x-\bar{x})}{2|\mathbf{x}-\mathbf{x}|^3} \qquad (|\mathbf{x}-\mathbf{x}| > R)$$

$$\mathbf{u}^{in} = \nabla\phi^{in} = -\mathbf{U}\frac{2(1-\kappa)}{2+\kappa} \qquad (|\mathbf{x}-\bar{\mathbf{x}}| < R) \qquad (1)$$

where $\mathbf{V} = \mathbf{U} + \mathbf{u}$ is the total velocity, $\mathbf{u}$ is the perturbation, $\bar{\mathbf{x}}(\bar{x}, \bar{y}, \bar{z})$ is the coordinate vector of the center and $\kappa = K/K_0$.

[10] Transport was analyzed in the past [*Dagan et al.*, 2003; *Fiori et al.*, 2003a] along the lines of *Eames and Bush* [1999]. A thin plume of uniform mass distribution is injected at $t = 0$ over a plane $x - \bar{x} = -L$ ($L \gg R$). Its subsequent motion was described in terms of $\mathbf{x} = \mathbf{X}(t; -L, b, \kappa)$, the trajectory of a particle originating at $x = -L$, $\rho_t = b$ at $t = 0$, where $\rho_t = [(y-\bar{y})^2 + (z-\bar{z})^2]^{1/2}$ is a transverse radial coordinate. The result of numerical integration of $d\mathbf{X}/dt = \mathbf{V}(\mathbf{X})$ is illustrated in Figure 1, reproduced from *Dagan et al.* [2003], which depicts snapshots of the plume at different t, for two values of $\kappa = K/K_0$. For a sufficiently large tU/R the plume shape stabilizes and it translates with velocity U. The residual $X_D(b, \kappa) = \lim_{t\to\infty}(X - Ut)$ is independent of time and it was used in order to characterize dispersion [*Eames and Bush*, 1999; *Fiori et al.*, 2003a; *Dagan et al.*, 2003].

[11] In contrast with the previous works, we model in P1 and here transport in terms of the traveltime of a particle from the injection plane to a control plane. The asymptotic traveltime residual τ_R is derived here from the equation

$$\tau_R(b,\kappa) = \lim_{L\to\infty}\left\{\int_{-L}^{L}\frac{dx}{V_x[x,\rho_t(x);\kappa]} - \frac{2L}{U}\right\} \qquad (L \gg R) \quad (2)$$

where $\rho_t = \rho_t(x)$ is the equation of a streamline originating at $\rho_t = b$ for $x = -L$. In words $\tau_R = -X_D/U$ is the delay or advance of the traveltime of a particle with respect to the mean time and it becomes independent of L for L larger than a few radii R (see Figure 1). While the derivation of τ_R requires a numerical integration [see *Fiori et al.*, 2003b], a simple analytical expression can be obtained for $\tau_M(\kappa) = \tau_R(0, \kappa)$, along the central streamline $b = 0$ by using (1) as follows

$$\tau_M(\kappa) = \tau_M^{in}(\kappa) + \tau_M^{ex}(\kappa) \tag{3}$$

$$\frac{U\,\tau_M^{in}(\kappa)}{R} = \int_{-R}^{R} \frac{d(x/R)}{1 + (u^{in}/U)} - 2 = \frac{4(1-\kappa)}{3\kappa} \tag{4}$$

$$\begin{aligned}\frac{U\,\tau_M^{ex}(\kappa)}{R} &= \lim_{L\to\infty}\left\{2\int_R^L \frac{d(x/R)}{1 + [u^{ex}(x,0,0)/U]} - 2\left(\frac{L}{R} - 1\right)\right\} \\ &= \frac{4(1-\kappa)}{2+\kappa}\int_1^\infty \frac{dx}{x^3 + 2(\kappa-1)/(2+\kappa)} \\ &= \Re\left[\frac{2}{3c^{1/3}}\left(\ln\left(1 + c^{-1/3}\right) + i^{4/3}\ln\left(1 + i^{4/3}/c^{1/3}\right)\right.\right. \\ &\quad \left.\left. - i^{2/3}\ln\left(1 - i^{2/3}/c^{1/3}\right)\right)\right]\end{aligned} \tag{5}$$

with τ_M^{in} and τ_M^{ex} pertaining to the part of the streamline within and outside the sphere, respectively; $i = (-1)^{1/2}$, $c = (2+\kappa)/(2(\kappa-1))$.

[12] For κ close to the extreme value $\kappa \to 0$ τ_M is dominated by the residual of the traveltime in the interior of the inclusion $\tau_M^{in}(\kappa)$ (4) that tends to infinity. Conversely, for $\kappa \to \infty$ the residual traveltime tends to $\tau_M \approx -2.577R/U$. This asymmetry of X_D (displayed in Figure 1) and of τ_M is the key to understanding the tailing of the traveltime distribution discussed in P1 and analyzed in detail in the sequel.

[13] For the purpose of characterizing the spreading of the plume we have found in the past [*Fiori and Dagan*, 2003] that the distribution of τ_R (2) can be simplified considerably. First, we found that the contribution to τ_R of the streamlines that circumvent the inclusion is negligible. The contributing streamlines which cross the inclusion originate from a disk of radius b. Its area $A_L = \pi b^2$ is related through the continuity equation to the central area of the sphere $A = \pi R^2$ by

$$\frac{A_L}{A} = \frac{V^{in}}{U} = \frac{3\kappa}{2+\kappa} \tag{6}$$

where $V^{in} = U + u^{in}$ (1).

[14] Furthermore, *Fiori and Dagan* [2003] found that τ_R can be expressed in an approximate manner in terms of τ_M by the simple relationship

$$\tau_R(\rho,\kappa) = \tau_M(\kappa)\frac{l(\rho)}{2R}, \quad l = 2\left(R^2 - \rho^2\right)^{1/2} \qquad (0 < \rho < R) \tag{7}$$

where l is the segment of the straight streamline within the sphere and ρ is a radial coordinate in the central plane $x = \bar{x}$. Equation (7) is exact for the central streamline $\rho = 0$ and for the contribution to the residual of the traveltime $\tau_R^{in}(\rho)$ within the sphere, since V^{in} is constant.

2.2. Traveltime pdf for Transport Past an Inclusion Belonging to an Ensemble

[15] In line with our previous work (see Introduction) the motion of a particle through the dense ensemble of inclusions is approximated by the sum of the effects of isolated inclusions of different, random, K. The interaction between inclusions is taken into account in an approximate manner by selecting $K_0 = K_{ef}$ i.e., $\kappa = K/K_{ef}$. The latter is determined by the self-consistent or effective medium theory [*Milton*, 2002] as a solution of the integral equation $\int (K_{ef} - K)/(2K_{ef} + K)\, f(K)\, dK = 0$, with $f(K)$ the pdf of K (hereinafter the notation $f(\cdot)$ denoted the pdf of the argument). It was found to provide a very accurate value for a lognormal distribution and the densest packing of spheres [*Janković et al.*, 2003a].

[16] Our aim is to derive the pdf of the traveltime of a solute particle between $x = 0$ and x that moves over a large number M of inclusions of different, random, κ_j and $\bar{\mathbf{x}}_j$ ($j = 1, \ldots M$). This is written as

$$\tau(x) = T + \sum_{j=1}^{M} \tau_{Rj} \quad ; \quad T = \frac{x}{U} \tag{8}$$

where the residuals τ_{Rj} are random variables associated with the various inclusions crossed by the particle. Our approximation is to regard them as independent and to determine them for each inclusion separately, along the lines of the preceding subsection. We also assume that $x \gg R$, so we can adopt the asymptotic $\tau_R(\rho, \kappa)$ (2) for a generic inclusion that is not close to the injection plane $x = 0$.

[17] The randomness of τ_{Rj} stems from two independent factors: (1) the position of the particle within the area A_L and correspondingly in the central plane A of the inclusion and (2) the value of κ_j. Conditioning on a fixed value of the latter, makes the randomness of the trajectory within the sphere manifest as randomness of the segment of crossing l (7). Assuming that the particle originates at equal probability from any point within A_L, the same is true for any point in A. Hence we can write for the pdf of l, $f(l)\, dl = dA/A = (2\pi\rho d\rho)/(\pi R^2)$ and with $l = 2(R^2 - \rho^2)^{1/2}$ we get

$$f(l) = \frac{l}{2R^2} \qquad (0 \le \rho \le R) \tag{9}$$

[18] However, the probability of crossing A depends on the presence of the particle within the wake A_L, i.e., it is proportional to $A_L/A = V^{in}/U$ (6). Summarizing, the pdf of τ_R, conditioned on the value $K_j = K$, is given by using (7), as

$$\begin{aligned} f(\tau_R|\kappa)\, d\tau_R &= \frac{V^{in}(\kappa)}{U} f(l)\, dl \ \text{ i.e.} \\ f(\tau_R|\kappa) &= \frac{V^{in}(\kappa)}{U}\frac{l}{2R^2}\frac{dl}{d\tau_R} = 2\frac{V^{in}(\kappa)}{U}\frac{\tau_R}{\tau_M(\kappa)\,|\tau_M(\kappa)|} \\ &\quad (0 \le |\tau_R| \le |\tau_M(\kappa)|) \end{aligned} \tag{10}$$

and it can be checked that $\int_0^\infty f(\tau_R)\, d\tau_R = 1$ (since in equation (10) $\int_0^\infty (V^{in}/U)\, f(\kappa)\, d\kappa = 1$ by the definition of

K_{ef}). It is emphasized that τ_R can be positive or negative, the sign being the same as that of τ_M.

[19] We are now in a position to derive the marginal pdf of τ_R. Toward this aim we invert first the relationship $\tau_M(\kappa)$ (3) as $\kappa = \eta(\tau_M)$ with $0 < \kappa < \infty$. Then we get finally, by observing that for a given $|\tau_R|$ in (10) the contribution to the integral over K is different from zero only for $|\tau_M(\kappa)| > |\tau_R|$,

$$f(\tau_R) = \int_0^\infty f(\tau_R|\kappa) f(K)\, dK = 6\tau_R \int_0^{\eta(\tau_R)} \frac{\kappa}{2+\kappa} \frac{1}{\tau_M^2(\kappa)} f(\kappa)\, d\kappa \quad (\text{for } \tau_R > 0)$$
$$f(\tau_R) = \int_0^\infty f(\tau_R|\kappa) f(K)\, dK = -6\tau_R \int_{\eta(\tau_R)}^\infty \frac{\kappa}{2+\kappa} \frac{1}{\tau_M^2(\kappa)} f(\kappa)\, d\kappa \quad (\text{for } \tau_R < 0) \tag{11}$$

[20] The integrals in (11) can be rewritten in terms of $Y' = \ln(K/K_G)$, with $f(\kappa)d\kappa = f(Y')\, dY'$, $\kappa = \zeta \exp(Y')$ and $\zeta = K_G/K_{ef}$, as follows

$$f(\tau_R) = 6\tau_R \zeta \int_{-\infty}^{\ln[\zeta\eta(\tau_R)]} \frac{e^{Y'}}{2+\zeta e^{Y'}} \frac{1}{\tau_M^2(\kappa)} f(Y')\, dY' \quad (\tau_R > 0)$$
$$f(\tau_R) = -6\tau_R \zeta \int_{-\infty}^{\ln[\zeta\eta(\tau_R)]} \frac{e^{Y'}}{2+\zeta e^{Y'}} \frac{1}{\tau_M^2(\kappa)} f(Y')\, dY' \quad (\tau_R < 0) \tag{12}$$

[21] It can be shown from (11) that the mean of the residual τ_R is not equal to zero, resulting in a "drift", which is calculated as follows

$$d = \langle \tau_R \rangle = 2\zeta \int_{-\infty}^{\infty} \frac{e^{Y'}}{2+\zeta e^{Y'}} \tau_M\left(\zeta e^{Y'}\right) f(Y') dY' \tag{13}$$

[22] The complete solution of τ_R (2) satisfies the relationship $\int_0^\infty \tau_R(b, \kappa)\, bdb = 0$ and no drift were present should we have employed it. The simplified solution (12) does lead to the drift, because of the neglect of the impact of the streamlines exterior to the inclusion which is implicit in the approximation (7). However, *Dagan and Fiori* [2003] observed that the exterior contribution has negligible influence on higher-order moments of τ_R, although it slightly affects $\langle\tau\rangle$. Nevertheless, for consistency we shall subtract d (13) from $T = x/U$ in the pdf of τ.

2.3. Derivation of the pdf of the Traveltime to the Control Plane

[23] The traveltime τ (8) is the sum of the various τ_R experienced by the particle while moving through the composite system. Following the dilute approach, we assume independence of the τ_{Rj} in (8). As a consequence, the pdf of τ is simply obtained as the multiple convolution of $f(\tau_R)$. The number of convolutions M is a random number, because it depends on the particular path experienced by the solute particle. However, the coefficient of variation of M drops quickly with the CP distance x, such that we can assume $M \cong \overline{M}$. The latter is the average number of inclusions crossed by the particle, which is equal to $nx/\langle l\rangle$, where n the volume fraction and $\langle l\rangle = 4R/3 = 16I/9$ (9) is the mean segment covered by the particle inside inclusions. The above steps result in the following expression for $f(\tau, x)$, which is identical to the mass flux $\mu(\tau, x)$ (see P1, equation (2)) under ergodic conditions,

$$f(\tau, x) = f_{\tau_R}(\tau - T - d) * f_{\tau_R}(\tau - T - d) * \ldots \left(\overline{M} \text{ convolutions}\right) \tag{14}$$

[24] At this point it is worthwhile to mention that in principle the inclusions crossed by the injection plane $x = 0$ shall be treated differently from those in the bulk, depending on the injection mode. However, the weight V^{in}/U attached to the probability of a particle to cross an inclusion of conductivity κ (10) precisely reflects the flux proportionality of the initial mass and there is no need to modify $f(\tau, x)$ (14), except for a different distribution of l in the first layer.

[25] By using Fourier transform (FT), equation (14) may be rewritten as follows

$$f(\tau, x) = \mathrm{FT}^{-1}\left[\tilde{f}_{\tau_R}^{\overline{M}}\right] \tag{15}$$

where $\tilde{f}\tau_R$ is the Fourier transform of $f(\tau_R)$. As mentioned before, by writing (14) we implicitly neglect the influence of the layer of inclusions crossed by the injection plane $x = 0$ on the distribution of τ_R. This influence, which in principle implies a change of $f(\tau_R)$ in the first term of the series (14), soon vanishes after a few convolutions and we omit it for the sake of simplicity.

[26] The traveltime variance is easily calculated from (14), along the properties of convolution operator. The variance of τ is equal to

$$\sigma_\tau^2 = N\sigma_{\tau_R}^2 = \sigma_{\tau_R}^2 \frac{nx}{\langle l\rangle} \tag{16}$$

The linearity of σ_τ^2 with x stems from the use of (11) for representing the τ_R distribution everywhere, including the injection zone, as previously explained. The variance $\sigma_{\tau_R}^2$ is given by

$$\sigma_{\tau_R}^2 = \langle \tau_R^2 \rangle - \langle \tau_R \rangle^2 = \frac{3}{2}\int_0^\infty \frac{\kappa}{2+\kappa} \tau_M^2(\kappa) f(K)\, dK - \langle \tau_R \rangle^2$$
$$= \frac{3}{2}\int_0^\infty \frac{\kappa}{2+\kappa} \tau_M^2(\kappa) f(K)\, dK - d^2 \tag{17}$$

The longitudinal macrodispersivity is further calculated from (17) as $\alpha_{Leq} = U^2\sigma_\tau^2/(2x) = nU^2\sigma_{\tau_R}^2/(2\langle l\rangle)$, and the final expression is identical to expression (B4) obtained by *Fiori et al.* [2003b] after neglect of the small, lower-order term d^2

$$\alpha_{Leq} = \frac{9nU^2}{16R} \int_0^\infty \frac{\kappa}{2+\kappa} \tau_M^2(K) f(K)\, dK \tag{18}$$

[27] It is emphasized that α_{Leq}/I is a function of σ_Y^2 only, i.e., the transport is Fickian according to this criterion. This is a direct consequence of our requirement $x \gg I$, to permit neglecting in (8) the impact of the "boundary layer" adjacent to the injection plane $x = 0$ in which the use of the asymptotic τ_R (7) is not warranted.

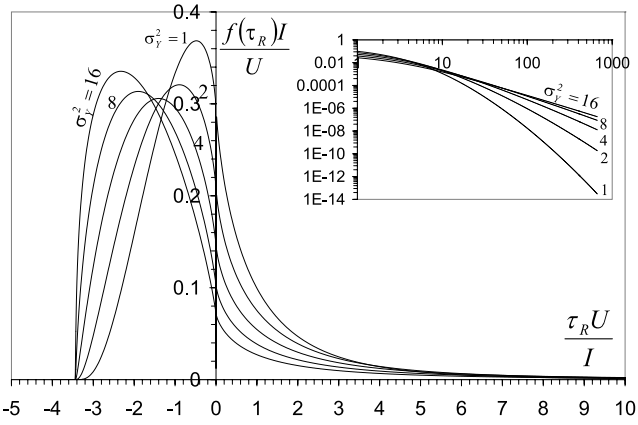

Figure 2. Distribution $f(\tau_R)$ (equation (12)) as function of τ_R for a few values of the log conductivity variance σ_Y^2.

[28] The simplified expression (18) has the following properties [*Fiori et al.*, 2003b]: (1) it leads to the well known first-order solution $\alpha_{Leq} = \sigma_Y^2 I_Y$ when $\sigma_Y^2 \ll 1$ and $x \gg I$, (2) it is equal to the dilute solution for $\sigma_Y^2 \gg 1$, (3) it differs from the complete self-consistent solution by a few percents.

3. Derivation of the Traveltime pdf for a Lognormal *K* Distribution

[29] The derivation of the traveltime pdf $f(\tau)$ is easily performed from (15). The procedure is as follows: (1) a lognormal distribution is adopted for $K = K_G \exp(Y')$, i.e., $f(Y') = [1/(2\pi\sigma_Y^2)^{1/2}]\exp(-Y'^2/2\sigma_Y^2)$; (2) $f(\tau_R)$ is derived through (12), which in most of the cases requires a numerical quadrature; (3) the Fourier transform f_{τ_R} is obtained numerically through fast Fourier transform (FFT), and (iv) finally $f(\tau)$ is obtained through inverse FFT of (15). The procedure is simple and typically takes a few minutes on a PC. Herein a few results of interest.

[30] We start from the distribution $f(\tau_R)$ (12), which represents the kernel of the sequence of convolutions (14) leading to $f(\tau)$. The distribution $f(\tau_R)$ is indeed central to the system response in terms of transport dynamics, and it is worth studying some of its features. Figure 2 depicts $f(\tau_R)$ (12) as function of τ_R, for a few values of the log conductivity variance σ_Y^2. The distribution of τ_R for $\sigma_Y^2 = 1$ displays some asymmetry, characterized by a relatively high flux of early arrivals ($\tau_R < 0$) and a relatively broad distribution of late particles ($\tau_R > 0$). The latter is manifested by the tail of the distribution, which is magnified in the inset of Figure 2. The skewness tends to disappear when $\sigma_Y^2 \to 0$, and $f(\tau_R)$ tends to $f(K)$, which is approximately Gaussian. Conversely, the asymmetry of $f(\tau_R)$ increases with σ_Y^2, as shown in Figure 2. The large σ_Y^2 curves are characterized by a significant shift of the main bulk of the pdf toward the negative τ_R region, which represents the fast solute arrivals. The latter tend to concentrate with time as σ_Y^2 grows, as emphasized by the increasing, nonmonotonous peak of $f(\tau_R)$. The concentration of fast arrivals may be caused by the relative decrease of the spatial variability of the high velocities, which determine the early arrivals distributions. In words, more and more fast preferential channels activate as σ_Y^2 grows, but the velocity variations in such channels do not increase dramatically. In contrast, the distribution of the late arrivals ($\tau_R > 0$ region) displays a considerable spread for increasing values of σ_Y^2. The significant tailing, which persists over a large timescale, is emphasized in the inset of Figure 2. The same features were observed in P1 when discussing the numerical results.

[31] We may conclude that an increase of the level of heterogeneity in the system results in a broader distribution of traveltime residuals for the kernel $f(\tau_R)$, with a sort of separation between the fast and late arrivals. The latter result in a persistent tailing of $f(\tau_R)$, which causes a significant departure from the Gaussian solution of transport after the multiple convolutions (14), the convergence to the normal solution being slow; this point is further discussed in the sequel.

[32] The solute flux $\mu(t, x)$, which is equal to the traveltime pdf $f(\tau; t, x)$ under ergodic conditions, results from the multiple convolution of the kernel $f(\tau_R)$, along (14–15). We represent in Figure 3 $\mu(t, x)$ as function of time for three fixed CP dimensionless distances $nx/I = 26.7$, 53.3,80.0 and for the two extreme cases $\sigma_Y^2 = 1$ and $\sigma_Y^2 = 16$. We observe that μ is very close to the normal distribution for $\sigma_Y^2 = 1$, while for $\sigma_Y^2 = 16$ the graphs display strong asymmetry and significant tailing. The departure from the

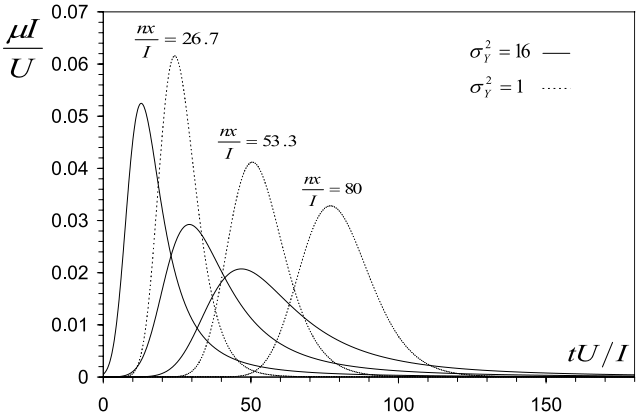

Figure 3. Ergodic solute flux $\mu(t; x)$ (equation (15)) as function of time for two extreme values of the log conductivity variance σ_Y^2 and for three control planes at x.

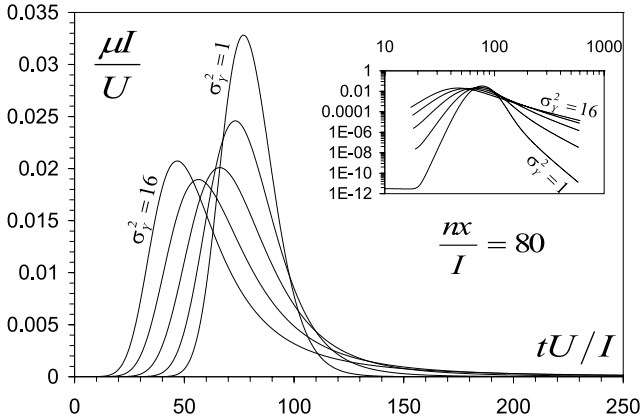

Figure 4. Ergodic solute flux $\mu(t; x)$ as function of time for a few values of the log conductivity variance σ_Y^2; the control plane is at $x = 80\ I/n$.

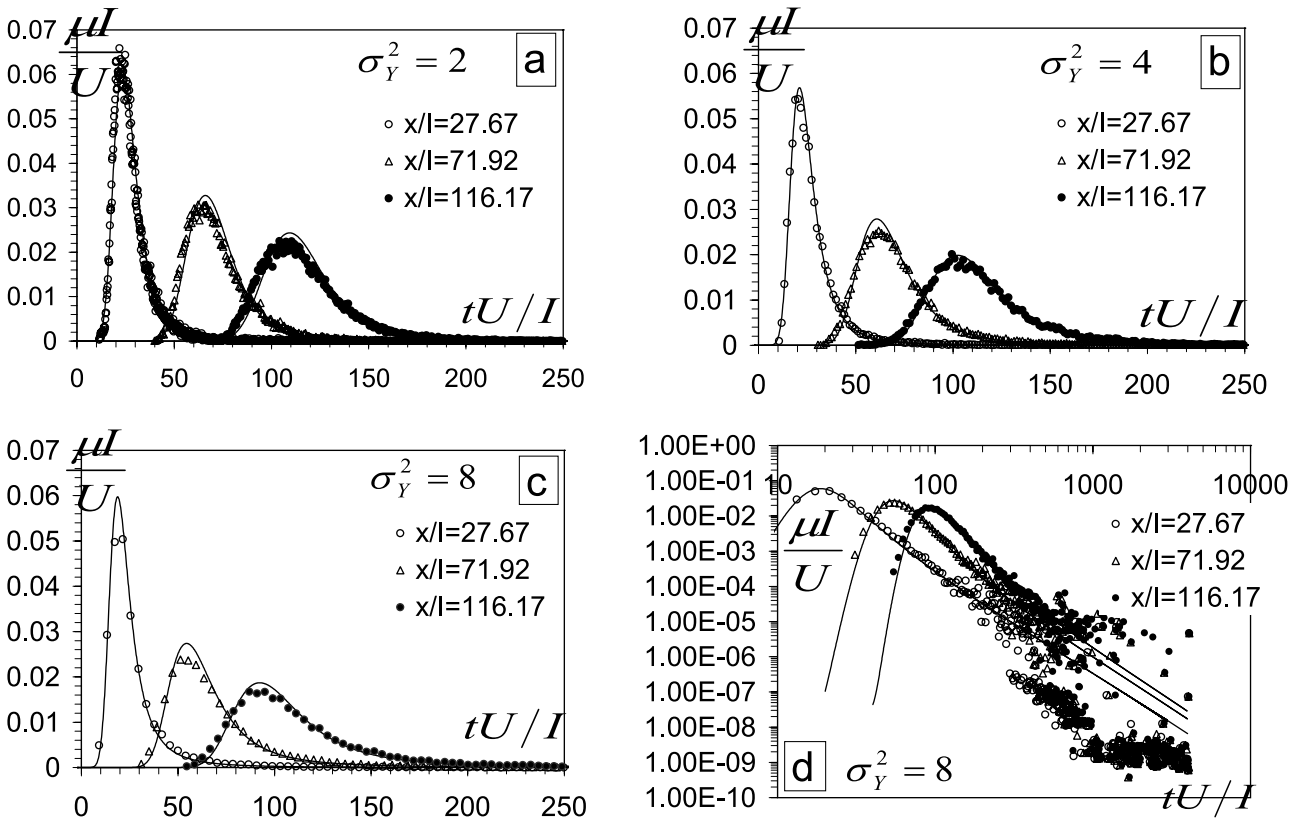

Figure 5. Solute flux μ (t; x) as function of time: comparison between theoretical (solid lines) and numerical (dots) solutions for three control planes, (a) $\sigma_Y^2 = 2$, (b) $\sigma_Y^2 = 4$, and (c) $\sigma_Y^2 = 8$. (d) Logarithmic plot of Figure 5c for the farthest control plane.

Gaussian limit for the largest σ_Y^2 is caused by the the high skewness and tailing of $f(\tau_R)$, as depicted in Figure 2, which makes the convergence to the normal limit (according to the central limit theorem) very slow.

[33] To further emphasize this effect, we represent in Figure 4 the solute flux μ (t, x) as function of t for a few values of σ_Y^2 for $x = 80I/n$. The departure from the Gaussian solution with increasing heterogeneity level is evident, with a pronounced early solute arrival (the time of the peak occurrence is almost halved). The other important feature is the persistent tailing, which is depicted in the inset of Figure 4. The "fat" tail of the traveltime distribution is determined by the solute retention in the inclusions of low permeability, the number of which increases with σ_Y^2.

4. Comparison With Numerical Simulations and the Impact of Ergodicity

[34] The theoretical solution derived above is compared now with the numerical results. These are given in P1, for the particular cases of σ_Y^2 = 2,4,8 and for a volume fraction $n = 0.7$.

[35] It is emphasized that the theoretical pdf $f(\tau, x)$ (15) was obtained by an ensemble statistics and it should be equal to the one realization μ (τ, x) of the numerical simulations of P1 only if the ergodic hypothesis is satisfied. This is precisely the topic we wish to examine next.

[36] Figure 5 displays the solute flux μ as function of time obtained by the numerical simulations and the present theoretical solution (solid lines). Three control planes are considered: x/I = 27.67, 71.92, 116.17. The agreement between the numerical and semianalytical solutions is very good, all the approximations notwithstanding, and the model is able to reproduce the transport features which were described in P1. We remind that there is no fitting parameter in the procedure, and all the parameters derive from the flow and conductivity setup: (1) the mean velocity U, (2) the inclusion radius R (equivalent to the integral scale $I = 3R/4$), (3) the log conductivity variance σ_Y^2 and (4) the volume fraction n.

[37] The theoretical solution seems to reproduce correctly the early arrivals and the prolonged tail. Again, the latter is related to the solute particles captured within inclusions of low K, in which the fluid velocity is very low and the residence time is very large. The accurate description of the tail, and the general good behavior of the theoretical model is attributed to the fact that the self-consistent model captures accurately the dominant term of the interior velocity [*Janković et al.*, 2003a, Figure 5]. However, the tail of the numerical μ is affected by great uncertainty at large times, as shown by Figure 5d which depicts in a log plot μ for the last CP, and for $\sigma_Y^2 = 8$. The dots begin to oscillate at around tU/I = 500 and the main reason is the lack of ergodicity, which was analyzed in P1. As discussed in P1, the ergodic problem becomes significant as the level of heterogeneity increases. Simply stated, as σ_Y^2 grows, a broader range of Y needs to be incorporated by the inclusions setup. The number of inclusions representing the

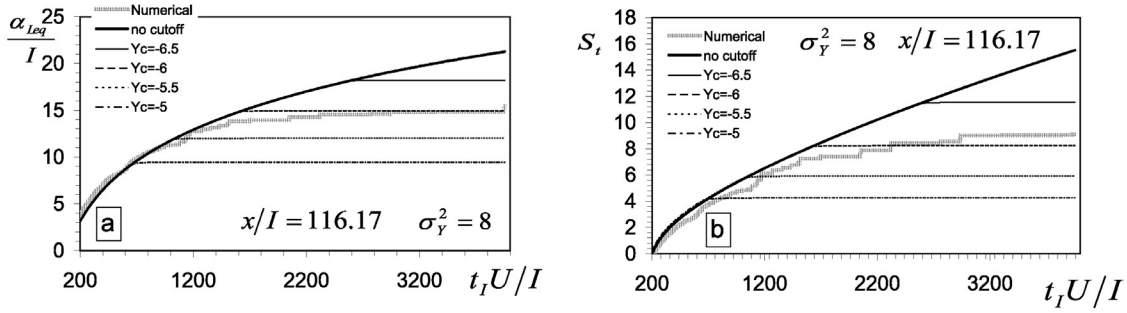

Figure 6. (a) Equivalent longitudinal dispersivity and (b) the travel time skewness as function of the integration time t_I for $\sigma_Y^2 = 8$ and $x/I = 116.17$: comparison between the numerical and the theoretical results for a few values of the log conductivity cutoff Y_c.

extreme values of Y in a finite plume might not be sufficient for a complete, ergodic representation of the medium structure. The same circumstance is likely to occur in applications, where the plume size may not be large enough to adequately sample all the states of the highly heterogeneous system. The nonergodic effect is visible in the logarithmic plot of Figure 5d, in which the dots spread is determined by the slowest particles experiencing the lowest-conductive spheres. In particular, the values around 10^{-9} are determined by arrivals of single particles or pairs.

[38] While $T = x/U$ is not affected by the tail, higher temporal moments, like the traveltime variance σ_τ^2, are strongly influenced by the tail and permit an assessment of the lack of ergodicity. We depict in Figure 6a the equivalent longitudinal macrodispersivity α_{Leq} as function of the integration time t_I (as defined in P1, equation (12)), for both the numerical simulations (thick line) and the theory (thin line, "no cutoff") for $\sigma_Y^2 = 8$. It is seen that the numerical and theoretical curves behave similarly up to, say, $t_I U/I = 1300$. After that limit, the two curves branch out, and the numerical one tends to level off. The theoretical curve continues to grow, and $\alpha_{Leq}(t_I)$ stabilizes after the huge time $t_I U/I = O(10^5)$ at the very large value 77.2 I (for the dependence of α_{Leq} (18) on σ_Y^2, see *Fiori et al.* [2003b]). The cause of this effect can be better understood from the examination of Figure 5d, in which the mass flux is represented on a logarithmic scale. While $f(\tau; t, x)$ and $\mu(t, x)$ start to differ only for a mass flux of the order of 0.001 of its maximum, the large observation time at which this happens has a significant impact on temporal moments.

[39] Since the macrodispersivity is affected considerably by the μ tail, its derivation and use is bound to be very problematic in field applications in highly heterogeneous formations, as discussed in P1. Thus characterization of transport through macrodispersivity may be unpractical in such cases.

[40] We may approximately account for the lack of ergodicity by introducing in the theoretical model a cutoff in the log conductivity field experienced by the plume. In particular, a lower cutoff Y_c can be easily introduced in (12), such that $f(\tau_R) = 0$ when $Y < Y_c$. The cutoff takes care of the inadequate sampling, caused, for instance, by the existence of an insufficient number of inclusions within a certain class of conductivity. Preliminary analysis of the conductivity field adopted in the numerical simulations indicated that the number of spheres having Y less than approximately -6 was highly oscillatory, leading to a probable cutoff around that value. In Figure 6a we represent α_{Leq} as function of the integration time t_I for a few values of the cutoff Y_c. It is seen that all the cutoff curves branch out from the ergodic one, similar to what happens in the numerical model. In particular, the cutoff value is around that indicated by the preliminary analysis of conductivity mentioned above. Similar considerations can be drawn for the skewness, illustrated in Figure 6b, which is even more affected by the tail. We emphasize that the impact of the tail and the lack of ergodicity are felt mainly in highly heterogeneous formations, while at small to moderate σ_Y^2 results are less dependent on the cutoff and the temporal moments display a faster convergence with t_I.

[41] Another approach to apply a cutoff was proposed in P1, namely, by approximating the mass flux $\mu(t, x)$ by the Gaussian expression (equation (9) in P1) and by fitting U_{eq} and α_{Leq} by a least squares procedure. These resulting "empirical" parameters, that are denoted as $U_{eq,G}$ and $\alpha_{Leq,G}$ and are functions of σ_Y^2 and of x/I, are not dependent anymore on the tail. Furthermore, they lead to a good agreement between the bulk of the simulated mass flux and the Gaussian approximation (see Figure 3 of P1).

[42] A similar procedure can be applied to the theoretical $f_\tau(t, x)$ (15). Since the latter was found to be close to the simulated $\mu(t, x)$ (Figure 5), it is expected that the fitted parameters by the Gaussian approximation (equation (9) of P1) shall lead to similar values. This is indeed the case as illustrated by Figures 7a (for $U_{eq,G}/U$) and 7b (for $\alpha_{Leq,G}/nI$), where the solid lines depict the fit of equation (9) of P1 with the theoretical pdf of equation (14), for $x \gg I$. This is an encouraging result, since it permits one to obtain a simple and accurate representation of the bulk of the plume, based on the simple semianalytical solution. It is seen that unlike the ergodic α_{Leq}, the fitted one displays an "anomalous" behavior, depending on σ_Y^2.

5. Summarizing Discussion and Conclusions

[43] Transport of conservative contaminant in a three-dimensional, isotropic, heterogeneous aquifer is the topic of the present sequence. The medium description and a few conceptual issues brought up by accurate numerical simulations of flow and transport in highly heterogeneous formations are given in P1. The focus of this part is the derivation of traveltime pdf $f(\tau, x)$ which is equal to the relative solute flux $\mu(t, x)$ of an ergodic plume, i.e., one

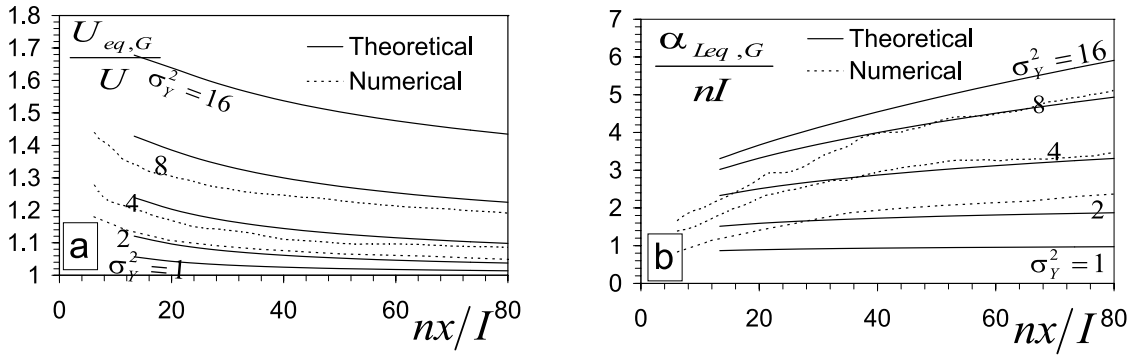

Figure 7. Dependence of the equivalent parameters (a) $U_{eq,G}/U$ and (b) $\alpha_{Leq,G}/nI$ on nx/I. Parameters were obtained by the Gaussian fitting of the numerical μ (t, x) and the semianalytical $f(\tau; t, x)$.

which is very large compared to the correlation scale of conductivity.

[44] The derivation of $f(\tau, x)$ is carried out with the aid of a simplified, semianalytical, model based on the "self-consistent" approximation applied to the transport problem [*Janković et al.*, 2003a; *Dagan et al.*, 2003; *Fiori et al.*, 2003a]. The model uses the simple solution of flow past an isolated spherical inclusion of arbitrary conductivity K that is submerged in a uniform matrix of conductivity K_0, with uniform flow U at infinity. The flow through the ensemble of spheres is approximated by the sum of the velocity perturbation fields associated with the different isolated spheres. The neglected interactions between neighboring inclusions are accounted for by replacing the matrix conductivity K_0 by the effective conductivity of the medium K_{ef}. Further simplifications are: the distribution of the asymptotic, residual traveltime τ_R of a thin plume moving over an inclusion is approximated in terms of the one on the central streamline τ_M; the total traveltime is the sum of independent τ_R associated with inclusions encountered by a solute particle; the number of such inclusions is deterministic and equal to its mean value. These simplifications render $f(\tau, x)$ as an approximation valid for $x \gg I$. The general and simple expression for $f(\tau, x)$ can be applied to any conductivity distribution, and some results have been obtained here for a lognormal K.

[45] The results obtained by the analytical model can be summarized as follows. The ergodic solute flux μ displays a Gaussian-like shape for weakly heterogeneous formations (say $\sigma_Y^2 < 1$), and solute transport can be predicted by the first-order theories of transport. As the log conductivity variance σ_Y^2 grows, μ displays two distinct features: (1) a thin and persistent, for a considerable time, tail, which is caused by solute mass moving very slowly in the medium, and (2) a shift of the solute flux peak, with a consequent shift of the main bulk of μ toward the lower t region, which is caused by fast, preferential flow paths in the system. As a result, the spread of μ, measured for instance through the longitudinal dispersion coefficient α_{Leq}, is considerable, and grows with σ_Y^2. This measure is determined mainly by the tail of μ, which in turn is caused by the low-conductive elements, the number of which increases with the log conductivity variance. Conversely, the effect of fast preferential flow on solute flux tends to stabilize with increasing σ_Y^2.

[46] It is found that the semianalytical model leads to an accurate solution, as compared with the numerical one. This is particularly true for highly heterogeneous formations and for the tail of the traveltime pdf, under the ergodic conditions to be discussed below. It is emphasized that the agreement was achieved with no fitting of parameters, and all of them are related to the conductivity setup and the mean flow conditions.

[47] The results of the two parts of this study permit us to draw conclusions about the main issues underscored by the title of the papers, as follows.

5.1. Ergodicity

[48] We could investigate this issue in P1 by examining the tail of numerically determined, one realization, mass flux μ (t, x) and the impact of reducing the plume size on its behavior. The issue was further clarified by the comparison with the traveltime pdf $f(\tau, x)$, which was determined here by an ensemble approach.

[49] The somewhat surprising finding was that even the plume of the large transverse initial area $A_0 = 2000I^2$ examined in P1, is not ergodic for large σ_Y^2. This is in variance with previous works [e.g., *Valocchi*, 1990; *Dagan*, 1991] that dealt primarily with weakly heterogeneous formations. The main conclusion is that the statistics of the tail of μ (t, x) is highly dependent on the degree of heterogeneity (σ_Y^2), on the plume transverse size (A_0), on the distance between the control and the injection plane (x/I) and on the observation time t. We have found a simple explanation of this effect: the presence of blocks of low K, in which solute particles are "stuck" for a long time. The number of such blocks depends obviously on σ_Y^2 and on the volume of the formation swept by the plume.

[50] Under ergodic conditions, and based on the traveltime pdf $f(\tau, x)$ of this part, it was found that the second temporal moment σ_τ^2 grows linearly with x (for $x/I \gg 1$). Hence the associated macrodispersivity $\alpha_{Leq} = \sigma_\tau^2 U^2/2x$ is independent of x, i.e., α_{Leq}/I is a function of σ_Y^2 solely and transport can be regarded as Fickian by this criterion. This is however a purely theoretical result, of little relevance to transport of finite plumes in highly heterogeneous formations, for a few reasons: the mass flux in the tail is very low, possibly below detection limit and is influenced by diffusion; the observation time is huge and the required plume size is very large, beyond the one expected in applications. These findings indicate that prediction of the tail in applications is quite problematic.

[51] On the positive side, the arrival of the bulk of the solute plume, as reflected by the early time μ, is less

subjected to fluctuations. It can be predicted accurately with the aid of the simple, semianalytical model of this part, provided a cutoff is applied at large t. The selection of such a cutoff may depend on the above consideration (an indirect approach is recalled in the following subsection).

[52] While the cutoff has a small impact on the mean traveltime, it affects considerably the second and higher temporal moments, making the ergodic α_{Leq} of little use for transport in highly heterogeneous formations.

5.2. Gaussianity

[53] While the mass flux and the associated BTC are of a Gaussian-like shape for weakly heterogeneous formations, μ becomes highly skewed with increasing σ_Y^2 (at a fixed x), while the peak is shifted to earlier arrival times. As found in here, Gaussianity is eventually reached under ergodic conditions, but for extremely large x/I, making this again of limited use in applications. Hence modeling of dispersion by the common ADE may lead to erroneous results, if the ergodic α_{Leq} is employed in the ADE.

[54] Still, if a cutoff is carried out at times t_I, for which most of the plume (say 95% and more) has crossed the control plane, the mass flux μ ($t < t_I$, x) is well approximates by a Gaussian-like shape. The latter is achieved by fitting either the numerically simulated mass flux or the semianalytical pdf of traveltime, by adjusting the two equivalent parameters $U_{eq,G}$ and $\alpha_{Leq,G}$. While $U_{eq,G}$ is somewhat larger than U (Figure 7a), $\alpha_{Leq,G}$ (Figure 7b) is considerably smaller than α_{Leq}, the differences decreasing with diminishing σ_Y^2. To illustrate this important point, we refer to Figure 6a, which shows that based on the traveltime distribution, for $x/I \simeq 116$ and for an observation time $t_I U/I = 3800$, the macrodispersivity $\alpha_{Leq}/I \simeq 20$, while the asymptotic value is $\alpha_{Leq}/I \simeq 77$. In contrast, the value obtained by the Gaussian fitting (Figure 7b) for the same $\sigma_Y^2 = 8$ and x/I is $\alpha_{Leq,G}/I \simeq 3.4$.

[55] The equivalent parameters can be determined from the simple semianalytical approximate solution, though the latter can be used directly after a cutoff has been performed.

[56] As mentioned already in P1, these fitted parameters are nonlocal as they depend on the distance from the source.

5.3. Anomalous Behavior

[57] The model permits us to describe the occurrence of anomalous transport, the latter being defined here as the circumstance under which macrodispersivity grows unbounded with time and the central limit theorem does not hold [*Bouchaud and Georges*, 1990]. According to our theoretical model, anomalous transport occurs only under the following conditions: (1) the conductivity distribution $f(K)$ is fat-tailed and "broad", with unbounded high-order moments (e.g., the Levy distribution), or (2) the distribution of R is power law, such that the integral scale of K is unbounded. In both cases, the multiple convolution of the kernel does not converge to the Gaussian limit, and therefore the central limit theorem does not hold anymore. In the literature, the impact of an unbounded integral scale of $Y = \ln K$ has been investigated for weak heterogeneity [*Glimm and Sharp*, 1991; *Glimm et al.*, 1993; *Dagan*, 1994; *Di Federico and Neuman*, 1998]. The more general cases are the same as the ones identified in the past by the scientific literature on the subject [see, e.g., *Bouchaud and Georges*, 1990]. The principal factor causing departure from the Gaussian limit is the persistent tail, which may vanish or not after the convolutions depending on the original structure of $f(K)$ and the derived kernel $f(\tau_R)$. It must be noted, however, that it is generally hard to distinguish between genuine anomalous and "normal" (but tailed) dispersion, especially in practical applications where other sources of uncertainty come into play (e.g., sampling and measurement errors). In fact, tendency to Gaussianity can be so slow that a clear distinction between the two mechanisms is not possible and perhaps almost irrelevant in applications, as mentioned in the preceding discussion. Consider for example the tail of $f(\tau)$ for $\sigma_Y^2 = 16$, as represented in the inset of Figure 4: the tail's behavior seems power law like, indicating thus anomalous transport. This is definitely not the case, because for a lognormal K of quickly decaying correlation (Figure 2 of P1) and finite integral scale, the central limit theorem always hold and the tail follows an exponential law. This should act as a warning against inaccurate and "qualitative", i.e., not related to the conductivity structure, interpretations of the BTC tail.

[58] Summarizing, we have taken advantage of the simple semianalytical model in order to acquire a better understanding of the mechanism of transport and of the limitations of numerical simulations. The model can be used as a simple tool toward predicting transport in heterogeneous formations, avoiding the use of macrodispersion or other related quantities and the Gaussian assumption. We emphasize again that the model is based on the ergodic assumption, which may not be fulfilled in applications dealing with high σ_Y^2. However, the lack of ergodicity mainly manifests in the thin tail and at large times. Application of the model to anisotropic structures and nonergodic plumes, as encountered in applications, as well as its further simplification, are topics of future studies.

References

Benson, D. A., S. W. Wheatcraft, and M. M. Meerschaert (2000), Application of a fractional advection-dispersion equation, *Water Resour. Res.*, *36*, 1403–1412.

Berkowitz, B., and H. Scher (1995), On characterization of anomalous disperion in porous and fractured media, *Water Resour. Res.*, *31*, 1461–1466.

Bouchaud, J. P., and A. Georges (1990), Anomalous diffusion in disordered media: Statistical mechanisms, models and physical applications, *Phys. Rep.*, *195*, 127–229.

Cushman, J. H., and T. R. Ginn (1993), On dispersion in fractal porous media, *Water Resour. Res.*, *29*, 3513–3515.

Cushman, J. H., and T. R. Ginn (2000), Fractional advection-dispersion equation: A classical mass balance with convolution-Fickian flux, *Water Resour. Res.*, *36*, 3763–3766.

Dagan, G. (1979), Model of groundwater flow in statistically homogeneous porous formations, *Water Resour. Res.*, *15*, 47–63.

Dagan, G. (1991), Dispersion of a passive solute in non-ergodic transport by steady velocity fields in heterogeneous formations, *J. Fluid. Mech.*, *233*, 197–210.

Dagan, G. (1994), The significance of heterogeneity of evolving scales to transport in porous formations, *Water Resour. Res.*, *30*, 3327–3336.

Dagan, G., and A. Fiori (2003), Time-dependent transport in heterogeneous formations of bimodal structures: 1. The Model, *Water Resour. Res.*, *39*(5), 1112, doi:10.1029/2002WR001396.

Dagan, G., A. Fiori, and I. Janković (2003), Flow and transport in highly heterogeneous formations: 1. Conceptual framework and validity of first-order approximations, *Water Resour. Res.*, *39*(9), 1268, doi:10.1029/2002WR001717.

Di Federico, V., and S. P. Neuman (1998), Transport in multiscale log conductivity fields with truncated power variograms, *Water Resour. Res.*, *34*, 963–973.

Eames, I., and J. W. Bush (1999), Longitudinal dispersion by bodies fixed in a potential flow, *Proc. R. Soc. London, Ser. A.*, *455*, 3665–3686.

Fiori, A., and G. Dagan (2003), Time-dependent transport in heterogeneous formations of bimodal structures: 2. Results, *Water Resour. Res.*, *39*(5), 1125, doi:10.1029/2002WR001398.

Fiori, A., I. Janković, and G. Dagan (2003a), Flow and transport through two-dimensional isotropic media of binary conductivity distribution, part 1. Numerical methodology and semi-analytical solutions, *Stochastic Environ. Res. Risk Assess.*, *17*, 370–383.

Fiori, A., I. Janković, and G. Dagan (2003b), Flow and transport in highly heterogeneous formations: 2. Semianalytical results for isotropic media, *Water Resour. Res.*, *39*(9), 1269, doi:10.1029/2002WR001719.

Glimm, J., and D. H. Sharp (1991), A random field model for anomalous diffusion in heterogeneous porous media, *J. Stat. Phys.*, *62*, 415–424.

Glimm, J., W. B. Lindquist, F. Pereira, and Q. Zhang (1993), A theory of macrodispersion for the scale-up problem, *Transp. Porous Media*, *13*, 97–122.

Harvey, C., and S. M. Gorelick (2000), Rate-limited mass transfer or macrodispersion: Which dominates plume evolution at the Macrodispersion Experiment (MADE) site?, *Water Resour. Res.*, *36*, 637–650.

Hughes, B. D. (1996), *Random Walks and Random Environments*, Oxford Univ. Press, New York.

Janković, I., A. Fiori, and G. Dagan (2003a), Effective conductivity of an isotropic heterogeneous medium of lognormal conductivity distribution, *SIAM J. Multiscale Model. Simul.*, *1*(1), 40–56.

Janković, I., A. Fiori, and G. Dagan (2003b), Flow and transport in highly heterogeneous formations: 3. Numerical simulations and comparison with theoretical results, *Water Resour. Res.*, *39*(9), 1270, doi:10.1029/2002WR001721.

Janković, I., A. Fiori, and G. Dagan (2006), Modeling flow and transport in highly heterogeneous three-dimensional aquifers: Ergodicity, Gaussianity, and anomalous behavior—1. Conceptual issues and numerical simulations, *Water Resour. Res.*, *42*, W06D12, doi:10.1029/2005WR004734.

Milton, G. W. (2002), *The Theory of Composites*, Cambridge Univ. Press, New York.

Valocchi, A. J. (1990), Numerical simulation of the transport of absorbing solutes in heterogeneous aquifers, in *Computational Methods in Subsurface Hydrology*, edited by G. Gambolati et al., pp. 373–382, Springer, New York.

G. Dagan, Faculty of Engineering, Tel Aviv University, Ramat Aviv, 69978 Tel Aviv, Israel. (dagan@eng.tau.ac.il)

A. Fiori, Dipartimento di Scienza dell'Ingegneria Civile, Universita' di Roma Tre, Via Volterra 62, I-00146 Rome, Italy. (aldo@uniroma3.it)

I. Janković, Department of Civil, Structural and Environmental Engineering, State University of New York at Buffalo, Buffalo, NY 14260-4400, USA. (ijankovi@eng.buffalo.edu)